A combinatorial droplet microfluidic device integrated with mass spectrometry for enzyme screening

Journal:	*Lab on a Chip*
Manuscript ID	LC-ART-10-2022-000980.R2
Article Type:	Paper
Date Submitted by the Author:	08-May-2023
Complete List of Authors:	Ha, Noel; Lawrence Berkeley National Laboratory, Biological systems and engineering; Joint BioEnergy Institute, Onley, Jenny; Sandia National Laboratories; Joint BioEnergy Institute, Deng, Kai; Sandia National Laboratories; Joint BioEnergy Institute Andeer, Peter; Lawrence Berkeley National Laboratory Bowen, Benjamin; Lawrence Berkeley National Laboratory Gupta, Kshitiz; Lawrence Berkeley National Laboratory, Environmental Genomics and Systems Biology; Joint BioEnergy Institute, Kim, Peter; Sandia National Laboratories; Joint BioEnergy Institute Kuch, Nathaniel; University of Wisconsin-Madison; Great Lakes Bioenergy Research Center Kutschke, Mark; University of Wisconsin-Madison Parker, Alex; University of Wisconsin-Madison Song, Fangchao; Lawrence Berkeley National Laboratory Fox, Brian; University of Wisconsin-Madison; Great Lakes Bioenergy Research Center Adams, Paul; Lawrence Berkeley National Laboratory; Joint BioEnergy Institute de Raad, Markus; Lawrence Berkeley National Laboratory, Environmental Genomics and Systems Biology Division Northen, Trent; Lawrence Berkeley National Laboratory; Joint BioEnergy Institute

SCHOLARONE™
Manuscripts

ARTICLE

A combinatorial droplet microfluidic device integrated with mass spectrometry for enzyme screening

Noel S. Ha[a,b,1], Jenny R. Onley[a,c,1], Kai Deng[a,c], Peter Andeer[b], Benjamin P. Bowen[b], Kshitiz Gupta[a,b], Peter W. Kim[a,c], Nathaniel Kuch[d,e], Mark Kutschke[d], Alex Parker[d], Fangchao Song[b], Brian Fox[d,e], Paul Adams[a,b], Markus de Raad[b] , Trent R. Northen[a,b,2]

Mass spectrometry (MS) enables detection of different chemical species with a very high specificity; however, it can be limited by its throughput. Integrating MS with microfluidics has a tremendous potential to improve throughput and accelerate biochemical research. In this work, we introduce Drop-NIMS, a combination of a passive droplet loading microfluidic device and a matrix-free MS laser desorption ionization technique called nanostructure-initiator mass spectrometry (NIMS). This platform combines different droplets at random to generate a combinatorial library of enzymatic reactions that are deposited directly on the NIMS surface without requiring additional sample handling. The enzyme reaction products are then detected with MS. Drop-NIMS was used to rapidly screen enzymatic reactions containing low (on the order of nL) volumes of glycoside reactants and glycoside hydrolase enzymes per reaction. MS "barcodes" (small compounds with unique masses) were added to the droplets to identify different combinations of substrates and enzymes created by the device. We assigned xylanase activities to several putative glycoside hydrolases, making them relevant to food and biofuel industrial applications. Overall, Drop-NIMS is simple to fabricate, assemble, and operate and it has potential to be used with many other small molecule metabolites.

1. Introduction

Coupling microfluidic technologies with high specificity analytical methods is desirable for a wide number of biotechnological and pharmaceutical applications.[1,2] Most mass spectrometry methods coupled with microfluidics have focused on electrospray ionization (ESI) mass spectrometry.[2–7] However, there are several reports of coupling microfluidics with laser desorption ionization mass spectrometry which has potential for high-throughput and smaller sample volumes. Microfluidics coupled with matrix-assisted laser desorption ionization time-of-flight mass spectrometry (MALDI-TOF MS) is a powerful technique[8–12] although the required addition of matrix adds complexity including matrix-suppression that makes the detection of small molecules challenging. Lapierre et al. successfully coupled digital microfluidics with matrix-free laser desorption ionization mass spectrometry, but this method was low throughput.[13] Alternative methods that enable high-throughput and matrix-free mass spectrometry directly from a microfluidics devices are needed. For examples of coupled microfluidics and mass spectrometry techniques that are relevant to biotechnology, see recent reviews.[1,2,14]

One matrix-free laser desorption ionization mass spectrometry technique is nanostructure-initiator mass spectrometry (NIMS), a powerful technology for rapid and sensitive analysis of a variety of samples types[15] Samples are deposited onto nanostructured surfaces which have "initiator" molecules trapped within. Initiator molecules and analytes are released when irradiated with a laser, but the initiator does not ionize and thus do not interfere with sample detection as matrix would. NIMS is amenable to high-throughput applications since only small (nanoliter to microliter) sample volumes are required. One useful application of NIMS is the characterization of enzymes.[16,17] However, high-throughput methods for setting up enzymatic reactions and transferring them to the NIMS chip surface are desired. A device that integrates microfluidics with NIMS would enable reactions at nL volumes and further improve scale-up. Heinemann et al. developed a device (μNIMS) that excelled at droplet manipulation, but it was difficult to scale up due to the complexity of fluid handling and mechanical failure of the system.[18] Additionally, samples had to be premixed off chip, limiting the number of combinations that could be tested simultaneously. Combinatorial droplet microfluidics is a powerful method for rapidly testing many combinations simultaneously[19]. While μNIMS is useful for time series, creating a new device with combinatorial droplet microfluidics would enable the testing of many more combinations. Recently the Blainey lab reported a droplet

[a.]Joint BioEnergy Institute, Emeryville, CA, USA
[b.]Lawrence Berkeley National Laboratory, Berkeley, CA, USA
[c.]Sandia National Laboratories, Livermore, California, USA
[d.]University of Wisconsin – Madison, Madison, WI, USA
[e.]Great Lakes Bioenergy Research Center, Wisconsin Energy Institute, Madison, WI, USA

[1.]Authors contributed equally to this work.
[2.]Correspondance: trnorthen@lbl.gov

Please do not adjust margins
Lab on a Chip
Page 2 of 9

microfluidics device for spectroscopic imaging.[19,20] The device randomly combines oil-encapsulated droplets, making it particularly appealing for integrating with mass spectrometry due to its simplicity, passive loading, and ability to assemble and mix combinations of droplets. However, the previously published device analyzes the contents of intact droplets, while combining the device with surface-based mass spectrometry would require drying the droplets and depositing the contents onto the mass spectrometry surface.

This paper describes a new device (Drop-NIMS) where the Blainey lab droplet microfluidic design was adapted and coupled with NIMS to introduce mass spectrometry-based analysis. Here, Drop-NIMS was leveraged to sample the combinatorial space of enzymes and enzymatic targets (i.e., substrates). Compounds with unique masses (henceforth referred to as barcodes) were also included to track the droplets so that multiple substrates and enzymes could be tested simultaneously. Drop-NIMS facilitated the rapid pairwise combination and merging of droplets to initiate biochemical reactions. The oil that encapsulates the droplets evaporated and the samples were deposited by Drop-NIMS onto the NIMS chip for mass spectrometry imaging without requiring further sample handling and transfer (Fig. 1). Drop-NIMS was applied to assay the substrate specificity of glycoside hydrolases (GHs), enzymes relevant to multiple industries including food, household products, and biofuel production.[21–23] Five GHs and four substrates were screened with up to 90 replicates per combination. From this we found that Drop-NIMS can be used to characterize enzymes in a detailed manner, with relative ease of device construction and use and with future potential for high-throughput screening.

2. Materials and Methods

2.1 Microfluidic Droplet Assay Chip Design and Fabrication

The microwell array chip, similar to previously-published designs[19,20] (Fig. 1a), is made of a polydimethylsiloxane (PDMS) layer bonded on a glass slide. The PDMS layer contains an array of 1,120 microwells (32 rows by 35 columns) that are open to the air. Variations in the microwell array chip were created wherein the wells were in groups of one, two, three, or four cylindrical sub-wells. The sub-wells are approximately 145 μm in diameter to entrap droplets with a diameter of 110 μm to 130 μm. The microwells are spaced 500 μm apart to prevent cross contamination. The PDMS layer was made using photoresist molds (SU-8 2075, Microchem) fabricated on a silicon wafer by photolithography per manufacturer's recommended protocol (see Electronic Supplementary Information for more detail).

To enable microscope imaging and sealing of droplets against the MS surface, the PDMS layer (approximately 120-150 μm thick) was bonded on a glass substrate. While the heights of the wells were not completely uniform, the wells were appropriately sized such that the sub-wells accommodate only one droplet each. The PDMS was squeezed between glass slides

and the mold, clamped using 2 neodymium magnets (6.35 mm OD x 4.76 mm T, McMaster Carr), such that the features on the master came into contact with the glass slide to create through-hole membrane structures. A new PDMS chip was used for each oil phase experiment to avoid cross-contamination.
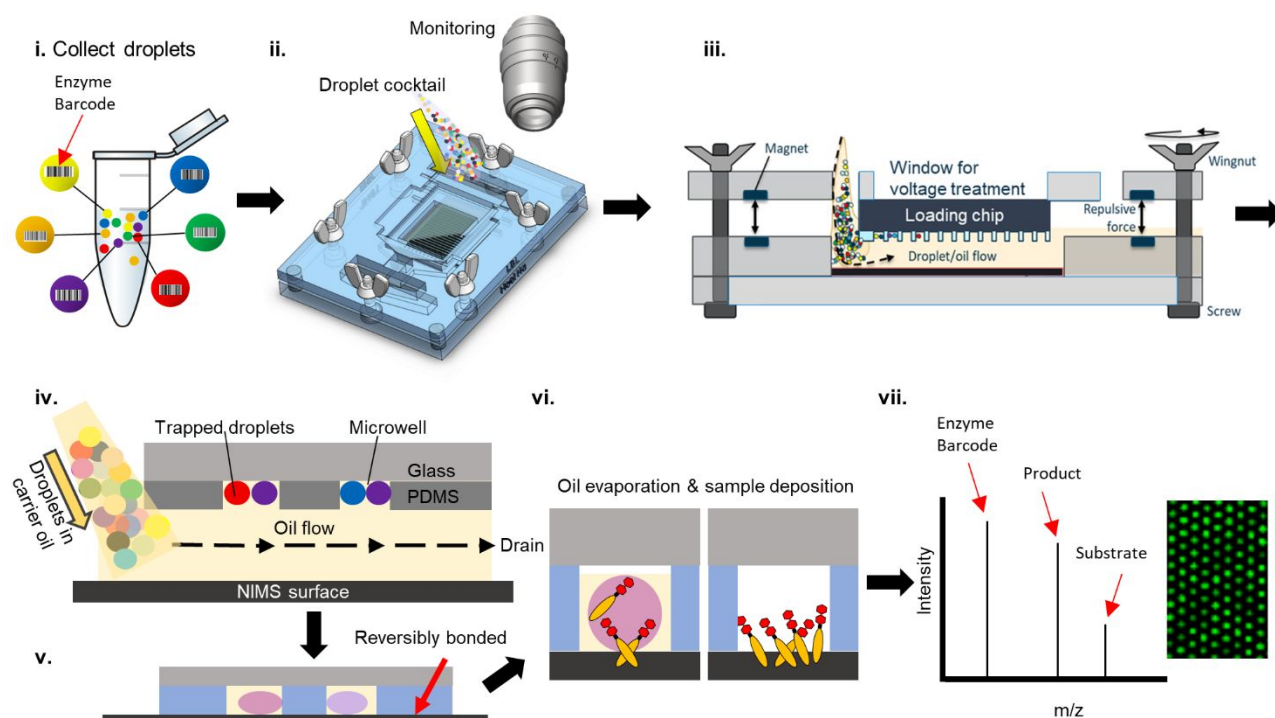
2.2 Device Assembly and Operation

A custom two-part apparatus was designed and 3D printed to hold the chips together and load the droplets (Fig. 1a). The microwell array chip was taped to the top part, which had a "window" for viewing and applying an electric field for merging the droplets. A NIMS chip was prepared as previously described[15] and taped to the bottom part (Fig. 1a). Nylon screws and wingnuts were used to prevent the applied electric field from being concentrated away from the chip while merging the droplets. The screws were tightened so that the microwell array chip was near but not sealed against the NIMS chip. The gap between the two parts, roughly 1 mm, was maintained by a balance between the wingnuts and repulsive force from the magnets.

Droplets were produced using the Bio-Rad QX200 Droplet Generator (Pleasanton, CA) according to manufacturer's instructions with a fluorocarbon oil (3M Novec 7500, $C_9H_5F_{15}O$) containing 2% 008-FluoroSurfactant (RAN Biotechnologies, Beverly, MA). Droplets were pooled to prepare a total of 200-400 μL suspension, which results in approximately 160,000 droplets. This is the number of droplets produced by one DG8 cartridge in the droplet generator and is much more than required to fill the 1,120 wells. The gap between the microwell array chip and the NIMS chip was primed with surfactant-free fluorocarbon oil before the injection of droplets. Droplets were loaded with the surfactant-free oil through the apparatus, flowing between the microwell array chip and the NIMS chip (Fig. 1b iii-iv; Supplemental Videos 1 & 2). The entire apparatus was gently tilted side to side to allow droplets to randomly fill the microwells, with up to 2,240 trapped droplets (two in each of the 1,120 microwells) in a double-well ("2x") droplet design. Excess droplets were washed away with the surfactant-free oil. The wingnuts were tightened until the microwell array chip, and the NIMS chip were sealed reversibly against one another (Fig. 1b.v). The droplets were merged via electrocoalescence, as described previously[19], by applying an electric field to the glass side of the microwell array chip for 10-20 seconds using a hand-held corona treater (BD-20AC, Electro-Technic Products, Chicago, IL).

a. Apparatus assembly
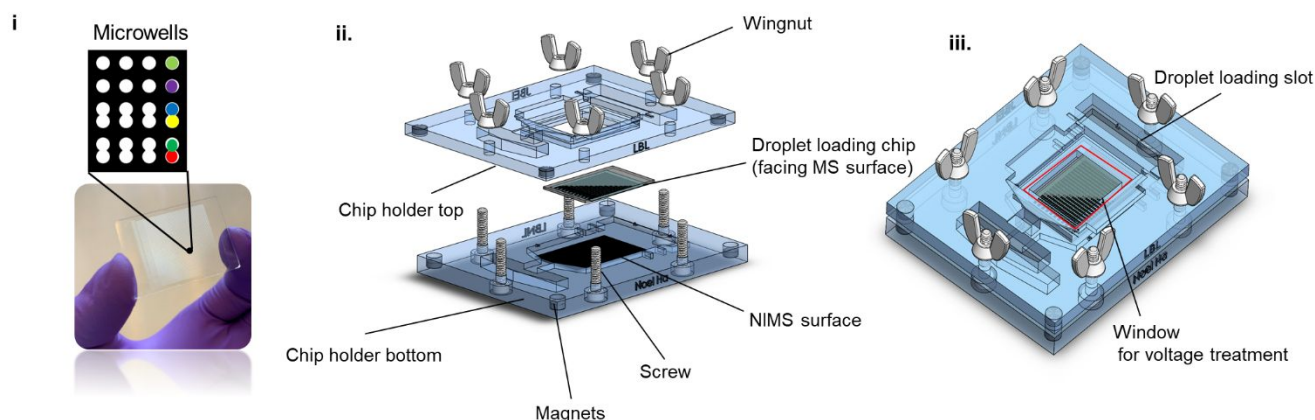
b. Device operation

Figure 1. Assembly and operation of microfluidics device. Not to scale. a) Assembly. i. The microwell array chip is composed of a glass layer and a thin PDMS layer containing microwells with 1, 2, 3, or 4 sub-wells. Inset contains example but does not show all wells. ii. The microwell array chip is attached to the top portion of the apparatus and the NIMS chip is attached to the bottom portion of the apparatus. iii. The screws are tightened so that the microwell array chip is close to the NIMS chip. b) Operation of Drop-NIMS. i. Micro-droplets are formed with the QX200 Droplet Generator (BioRad) and pooled. Each enzyme droplet contains a known compound to "barcode" the droplet. ii-iv. Droplet cocktail is transferred to Drop-NIMS (top, side views, and zoomed view). iii. Droplets are buoyant and randomly assemble into the microwells on the PDMS layer as they are washed through with oil. v. Screws are tightened against the repulsive force to reversibly seal the PDMS layer against the NIMS surface, and an electric field (not shown) is applied to merge droplets within the microwells. vi. Enzymatic reactions occur within the merged droplets. After 2 to 3 hours the carrier oil and sample buffer evaporate through the gas permeable PDMS and the droplet contents are deposited onto the NIMS surface. Orange ovals represent the NIMS tag and red hexagons represent G2 substrate. vii. The apparatus is disassembled, and the NIMS chip undergoes mass spectrometry imaging. The inset shows the OpenMSI image; the green spots represent detected signals.

Enzymatic reactions were initiated upon droplet merging while the chip remained sealed against the MS surface. The volatile carrier oil and solvent evaporated through the gas permeable PDMS layer, inducing sample deposition on the NIMS chip surface and halting the enzymatic reactions. After complete evaporation of oil and solvent, the NIMS chip was separated from the droplet microwell array chip for mass spectrometry imaging (MSI). For more details on device design, assembly, and operation, see Electronic Supplementary Information.

2.3 Cell-Free Protein Expression

Putative xylanases (a subtype of glycoside hydrolase) were identified through the National Center for Biotechnology Information Center (NCBI) Basic Local Alignment Search Tool (BLAST) by searching for sequences similar to known xylanase genes. Identified gene sequences were synthesized at the Joint Genome Institute (Berkeley, California) and cloned into pEU plasmid (plasmid of Ehime University, Matsuyama), a vector for cell-free expression.[24,25] Protein expression was performed as described previously[25] with sequential transcription-translation using wheat germ extract from Cell-Free Sciences (Yokohama, Japan). Briefly, the transcription reaction was performed using SP6 polymerase (Promega, Madison, WI, USA) and the

Please do not adjust margins
Lab on a Chip
Page 4 of 9

translation reaction was performed with a bilayered, diffusion-fed translation reaction. Protein production was quantified using band analysis on stain-free sodium dodecyl sulfate–polyacrylamide gel electrophoresis (SDS-PAGE) gels by comparison to a cell-free translation blank.

2.4 Preliminary Activity Screen and Cloning

Successfully expressed protein was screened for activity on 1,4-beta-D-mannan and barley beta glucan (low viscosity) from Megazyme (Bray, Ireland) and beechwood xylan from Sigma-Aldrich (St. Louis, Missouri); data not shown. Reactions were prepared with 10 mg/mL substrate, 4 µL cell-free translation reaction, and 0.1 M acetate buffer at pH 4.5, 5, or 6 to a final volume of 40 µL. Reactions were incubated at 32°C for 2 hours before centrifugation for 10 minutes at 4,000 rpm (3,283 x g) to pellet residual solids and the concentration of soluble reducing sugar was determined via the Pierce BCA Protein Assay Kit from Thermo Fisher Scientific (Waltham, Massachusetts). Briefly, 200 µL of BCA working solution and 10 µL of reaction supernatant were heated at 80°C for 30 min. Control samples contained either cell-free translation mixes only, substrate only, buffer only, or the cell-free translation blank and substrate. A glucose standard curve was used to convert absorbance units to mg/mL reducing sugar in solution.

2.5 Protein Expression and Purification

Four enzymes with sequence similarity to glycoside hydrolase family 43/subfamily 11 (GH43-11) enzymes were selected for characterization using NIMS analysis. Rosetta cells from Sigma Aldrich were transformed with plasmid containing the selected genes (pVP67K, N-terminal 8His TEV cleavable tag) and expressed via autoinduction as described previously.[26,27] Centrifuged cells were lysed via lysozyme and sonication; the lysate was centrifuged for 1 hour at 20,000 rpm (31,360 x g) and the supernatant was filtered through a 0.4 µm PES filter. Enzymes were purified from the filtered supernatant via nickel affinity chromatography on an Akta Start FPLC and subsequently desalted and concentrated. Concentrated enzyme solution was frozen in liquid nitrogen and stored at -20°C until later use. The source organisms and accession numbers are as follows: 43-Lact (*Lactobacillus kimchicus*, KRK47366.1), 43-Pedi (*Pediococcus acidilactici*, SJM45318.1), 43-Weis (*Weissella* sp., COI51269.1), and 43-Clos (*Clostridium* sp., SCJ27493.1).

2.6 Droplet Enzyme Reactions

Enzymatic reactions were performed at room temperature. A previously-characterized glycoside hydrolase, CelEcc-CBM3a,[28] and the four predicted glycoside hydrolases were chosen for proof-of-concept. Five NIMS-tagged model substrates were prepared as previously described[17] (Fig. S3), each with an ionizing moiety and an attached perfluorinated tail to aid in adherence to the NIMS chip: cellobiose (G2, 1101.3 or 1134.3 m/z), xylobiose (X2, 1041.3 m/z), xylotriose (X3, 1188.4 m/z) and xylotetraose (X4, 1320.4 m/z). Verapamil (454.3 m/z) and G2 were used to test the chip without enzyme. CelEcc_CBM3a,

a commercial xylosidase (Megazyme cat. # E-BXSEBP), a commercial glucosidase (catalog #49290-250 mg; Sigma-Aldrich), or buffer alone were used as controls. An equal number of substrate droplets and enzyme droplets were prepared to increase the number of wells that had at least one substrate droplet. Mass barcodes were included in enzyme droplets in order to track their locations on the chip. The following chemicals were used as mass barcodes from Cambridge Isotopes (Fig. S5): L-Carnitine:HCl, O-Dodecanoyl (unlabeled) (cat. # ULM-7199-0.1mg); L-Carnitine:HCl, O-Dodecanoyl (N-Methyl-D3) (cat. # DLM-8162-0.1mg); L-Carnitine:HCl, O-Dodecanoyl (N,N,N-Trimethyl-D9) (cat. # DLM-8215-0.1mg); L-Carnitine:HCl, O-Palmitoyl (unlabeled) (cat. # ULM-7738-PK); and L-Carnitine:HCl, O-Palmitoyl (N-Methyl-D3) (cat. # DLM-1263-0.01). Palmitoyl-13C16-L-carnitine hydrochloride (cat. # 644323-1.00mg) was purchased from Sigma. Enzyme droplets were generated with a concentration of 733 ug/mL enzyme and 250 µM barcode in 25 mM phosphate buffer, pH 6.0 (366.5 ug/mL enzyme and 125 µM barcode after droplet merging). Substrate droplets contained 1 mM substrate in 25 mM phosphate buffer, pH 6.0 (0.5 mM substrate after droplet merging).

2.7 Mass spectrometry Imaging (MSI) and Data Analysis

Sample deposition was confirmed using MSI. MSI was performed using an AB Sciex 5800 TOF/TOF mass spectrometer with a laser intensity of 2500-3000 over a mass range of 250–1500 Da. Each position accumulated 20 laser shots. The instrument was controlled using the MALDI-MSI 4800 Imaging Tool using a 50 µm step size between shots. Spectra were recorded in positive reflector mode. The instrument was calibrated using Anaspec Peptide Calibration mixture 1 (catalog #AS-60882; Anaspec, Fremont, CA).

For a quantitative analysis, OpenMSI (openmsi.nersc.gov) and the OpenMSI Arrayed Analysis Toolkit (OMAAT)[29] were used to identify wells displaying peaks for m/z values of interest. Due to the irregularly shaped sample spots (a common issue with the dried droplet method), the OMMAT script was modified to exclude pixels that did not contain any peaks of interest above a relative signal intensity of 100 (i.e., approximately four times the background noise) arbitrary units (au). The data were then analyzed with a customized script written with pandas[30,31] and Pingouin.[32]

3. Results & Discussion

3.1 Device Design and Operation

The main objectives of Drop-NIMS are to randomly combine droplets and to deposit the reaction products onto the NIMS chip surface. To accomplish random droplet combination, a microwell array chip was created as described earlier. After droplet loading, samples deposited onto the NIMS chip surface as the oil evaporated, and the apparatus was disassembled for NIMS chip imaging. Some PDMS wells were observed to not be completely through-hole, which can be explained by the

Please do not adjust margins

Lab on a Chip

Figure 2

Journal Name

LE

variability in the height of the pillars on the master. Moreover, the glass slide surface is not a perfect plane which can result in this observation as well. However, this was not observed to affect their ability to trap droplets.

The successful operation of Drop-NIMS was initially demonstrated with two molecules: NIMS-tagged cellobiose ("G2") and verapamil. Microwell array chips with 1x, 2x, 3x, and 4x microwells were used (Fig. S2a). Two different NIMS chips were used for G2 and for verapamil. Droplets were loaded into the assembled apparatus with the microwell array chip and the NIMS chip as described above. After the oil evaporated, the NIMS chip was separated and imaged using mass spectrometry imaging (MSI). MSI images demonstrated detection of G2 (Fig. S2b) and verapamil (Fig. S2c) with good signal to noise ratios, indicating that sample deposition onto the NIMS chip was successful.
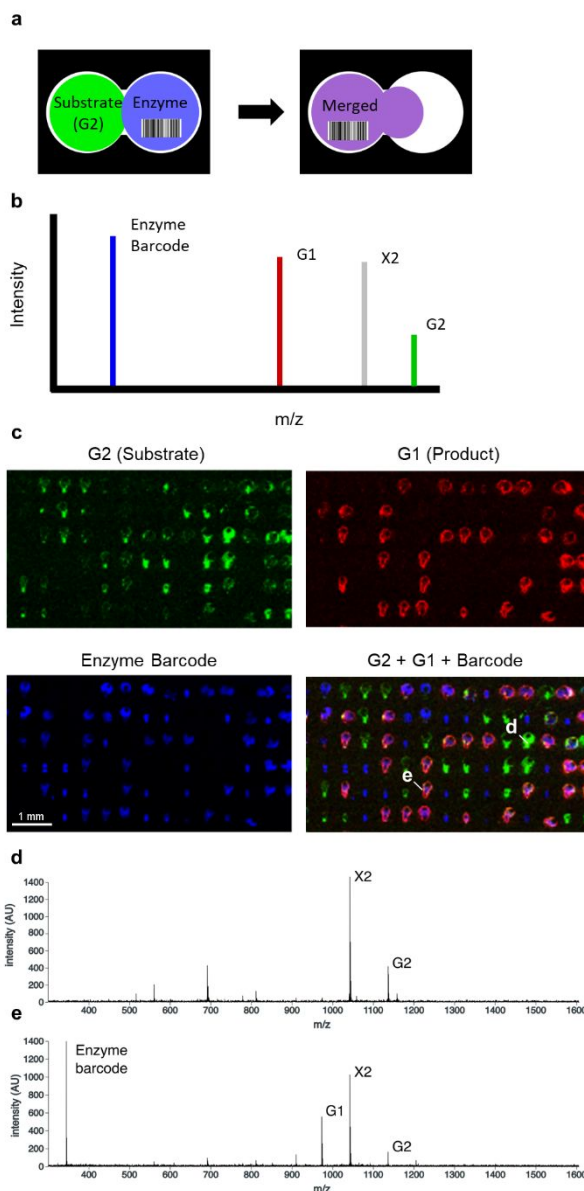

Figure 2. Droplet enzyme reaction with mass spectrometry barcode. a) Experimental setup schematic. Two types of droplets were prepared: one containing cellobiose (G2) and xylobiose (X2) and the other containing CelEcc_CBM3a enzyme with a barcode (DC-1). One possible combination is shown (other combinations are possible). b) Simulation of expected mass spectrometry spectrum with the enzyme substrate (G2), enzyme product (G1), and the barcode for tracking the location of enzyme droplets. c) OpenMSI images of NIMS chip after sample deposition. d-e) Sample spectrum from OpenMSI on spots without (d) and with (e) enzyme. Green indicates signal intensity at 1135 m/z (G2; substrate), gray indicates signal intensity at 1042 m/z (X2; substrate); red indicates signal intensity at 973 m/z (G1; product), and blue indicates signal intensity at 344 m/z (DC-1; barcode). Scale bar (1 mm) is common for all panels.

The device was then applied to enzymatic reactions, using droplets containing a previously characterized enzyme and droplets containing enzyme substrates. The enzyme was CelEcc_CBM3a, which is known to break down cellulosic compounds (which are composed of repeating glucose units),[28] and cellobiose (two glucose units; "G2") was used as the enzyme substrate (Fig. 2a). Droplets containing G2 also contained xylobiose (two xylose units; "X2") and were tracked by detection of X2, a substrate peak (G2) and/or the enzymatic product peak (glucose; G1).

An extra challenge with droplets lacking enzyme substrates (i.e., containing enzymes or buffer only) is that there is no distinct mass spectrometry signal in the selected mass range for

tracking the droplets. In order to track enzyme or buffer droplets, barcodes (chemical compounds of known mass) were added to identify the droplets. Thus, the location of an enzyme or buffer droplet could be determined by the detection of the mass barcode. Barcodes with the same structures but different isotopes are desirable since they ionize similarly in the mass spectrometer, but they have different masses. Barcodes in this experiment were various isotopes of palmitoyl carnitine or dodecanoyl carnitine (Fig. S5), which display high ionization efficiency on NIMS.

Drop-NIMS was loaded with droplets containing either CelEcc_CBM3a and barcode or G2 substrate. Substrate (G2), product (G1), and barcode (for tracking the enzyme) were detected (Fig. 2c-e). The G1 product was co-localized with the barcode, indicating that the conversion of G2 to G1 only occurred when enzyme was present. These results demonstrate that the device successfully randomly combined droplets, enabled subsequent enzymatic reactions, and then deposited the reaction products onto the NIMS chip surface, all while tracking the droplet content.

Drop-NIMS has several advantages over our previous NIMS-digital microfluidics device.[2,18] Enzymes and substrates can be loaded in separate droplets and randomly combined within the device, rather than premixing solutions. Randomized droplet combinations reduce manual pipetting and creates the potential for many more tested combinations. The simple design of the microwell array means many more samples can be added with minimal effort.

3.2 Application to Uncharacterized GH Enzymes

Drop-NIMS was applied to test multiple previously uncharacterized GH enzymes with G2 and X2 on a single chip. GH enzymes with similarity to enzymes in the GH43 family subfamily 11 (GH43-11; enzymes from Lactobacillus, Pediococcus, and Clostridium labeled 43-Lact, 43-Pedi, and 43-Clos, respectively) were tested. Characterized enzymes in the GH43-11 subfamily are known to target xylooligosaccharides (composed of repeating xylose [X] units) but not G2. Droplets containing 43-Lact, 43-Pedi, 43-Clos, CelEcc_CBM3a, and buffer alone were loaded along with "substrate droplets" containing a mixture of G2 and X2. Barcodes were included in droplets containing enzymes or buffer to facilitate droplet tracking. Two of the three uncharacterized enzymes (43-Lact and 43-Pedi) converted X2 substrate to X1 product, while no significant conversion of X2 was observed in droplets containing 43-Clos, CelEcc_CBM3a, or buffer (Fig. 3a; Tables S1-S3). However, the X2 data for 43-Clos was highly variable (Fig. 3a), with some data points having a high product:substrate ratio. This suggests that in some wells, 43-Clos hydrolyzed X2. It is possible that testing different reaction conditions (e.g., higher temperature or higher enzyme concentration) would result in a greater number of 43-Clos wells with hydrolyzed X2. As expected, only CelEcc_CBM3a converted G2 to G1 (Fig. 3b). The data for CelEcc_CBM3a was highly variable (Fig. 3a); however, on closer examination, the

data points that were far from the average had very low intensities (100-200 au) for both product and substrate peaks.

An additional GH enzyme from *Weissella*, 43-Weis, was chosen to further characterize its substrate specificity. A second chip was loaded with droplets containing 43-Weis, G2, and xylooligosaccharides (X2, X3, or X4). X2 and G2 were prepared within the same droplets whereas X3 and X4 were in separate
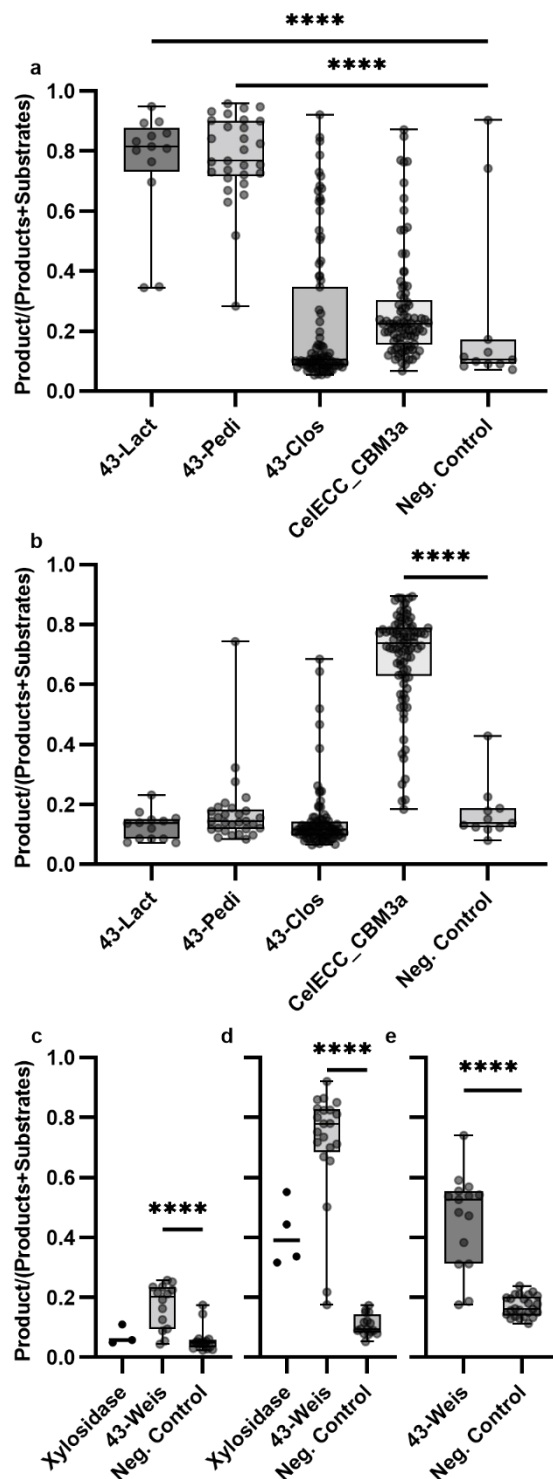

Figure 3. Rapid screening of glycosyl hydrolases with model hemicellulose compounds. Box and whisker plots. a-b) Results of a chip screening multiple enzymes (GH 43-Lact, 43-Pedi, and 43-Clos with CelEcc_CBM3a as a positive control and buffer as a negative control) with one substrate droplet type (containing a mix of G2 and X2). The proportion of products are shown for X2 conversion to X1 (a) and G2 conversion to G1 (b). c-e) Results of a chip screening one enzyme (GH 43-Weis) with commercial xylosidase as a positive control and beta-glucosidase as a negative control) with multiple substrate droplets (G2/X2 mix, X3, and X4). The proportion of products are shown for X2 conversion to X1 (c), X3 conversion to X1 and X2 (d), and X4 conversion to X1, X2, and X3 (e). Boxes show the 25th to 75th percentiles. The line within the box indicates the median. Whiskers indicate maximum and minimum. All samples were compared to the negative control; ****, P<0.0001. Xylosidase samples are shown as scatter plots (horizontal line indicates mean) due to low sample size (<5). Y-axes show the sum of the product peak intensities divided by the sum of products and substrate peak intensities (e.g., for X3 reactions, y-axis shows [X1+X2]/[X1+X2+X3]).

droplets. Droplets containing a commercial xylosidase (which hydrolyzes X2, X3, and X4) served as positive controls and droplets containing glucosidase (which does not hydrolyze X2, X3, or X4) served as negative controls. Like the previously tested enzymes, 43-Weis converted X2 to X1 (Fig. 3c; Tables S4-S6) but did not convert G2 to G1 (Fig. S4a). X3 was converted to X1 (Fig. 3d; Fig. S4 b), and X4 was converted to a mixture of X3 and X1 (Fig. 3e; Fig. S4e). As expected, the glucosidase hydrolyzed G2 to G1 but did not hydrolyze X2, X3, or X4 (Fig. 3c-e). Commercial xylosidase hydrolyzed X3 to X2 and X1, although there were only four replicates (Fig. 3d; Fig. S3d). No xylosidase and X4 combinations were observed. Overall, this experiment revealed that multiple substrates can be tested on a single chip. With this multi-substrate chip, barcodes were required for the substrate droplets in addition to the enzyme droplets to distinguish between X3 and X4 droplets (which can be hydrolyzed to the same products).

Drop-NIMS showed that three of the four tested enzymes have xylanase (X4, X3, and/or X2 hydrolysis) activity but not cellulase (e.g., G2 hydrolysis) activity. The results along with the protein sequence similarity to other GH43 family subfamily 11 proteins support the classification of 43-Lact, 43-Pedi, and 43-Weis as xylanases that target xylooligosaccharides.

3.3 Cross Contamination and Loading Efficiency

All compounds of interest (barcodes and NIMS-tagged enzyme substrates) were tractable by mass spectrometry and thus cross-contamination could be assessed by measuring signals between sample spots. Signal intensities of target compounds were typically below the threshold of 100 au in between samples, indicating that the sample was contained within the well (Fig. S6).

Although the loading and merging efficiencies of the microwell array chip was assessed in a previous publication,[19] both parameters can vary from chip to chip. The data from two chips are discussed in Figure 3; one contained multiple enzymes with one substrate droplet type (Fig. 3a and b), and the other contained one enzyme with multiple substrate droplet types (Fig. 3c-e). For these two chips, sufficient replication and minimal droplet breakage and cross-contamination was observed. Figure S7a shows the number of replicates for each chip. In both experiments, the number of substrate droplets was equivalent to the number of enzyme and buffer droplets, to ensure most wells receive substrate. The number of replicates of relevant reactions (i.e., ones that contained a substrate droplet and an enzyme or negative control droplet) were typically between 10 and 90 per combination type. However, there is some variability; on the chip for Figure 3c-e, there were very few spots containing xylosidase (eighteen) spots with xylosidase, and only seven of those had substrate). We speculate that the low replication of xylosidase droplets was due to insufficient mixing of the droplets prior to droplet loading. The need to thoroughly mix droplets while avoiding overmixing (which can lead to droplets breaking) is a limitation of our approach.

Figure S7b shows the number of droplets per doublet microwell for both chips, based on MS signal detection. The ideal number is two; one indicates that one sub-well was empty, and more than two indicates droplet breakage or cross-contamination (since the microwells can only accommodate two full-sized droplets). Only wells that contained signal were included in this analysis. Most of the wells for both chips had one or two droplets (94% for the first chip and 76% for the second chip), and wells containing mass spectrometry signals for more than two droplets were excluded from the analyses shown in Figure 3.

4. Conclusions

In conclusion, Drop-NIMS is a novel combination of NIMS and droplet microfluidics using standard photolithography techniques that can be used by the broader community to characterize enzymatic reactions. The research presented here demonstrates that the new device successfully deposits the contents of merged droplets directly onto NIMS chips. Mass spectrometry barcodes were included in order to track the contents of the droplets. Unlike a previous device that facilitated temporal experiments,[18] Drop-NIMS theoretically can provide higher throughput than previous NIMS approaches and capitalizes on the combinatorial power of droplet microfluidics. Although only a few reactions were tested here, Drop-NIMS has the potential for more than 1,000 simultaneous reactions and a requirement of only a small volume (nL) of enzymes and substrates per reaction. A multitude of droplets can be randomly combined for many combinations and replicates. One limitation of the platform is that, as with other droplet microfluidics platforms, droplets must be carefully manipulated to avoid breaking, but also must be thoroughly mixed to achieve good replication of all possible combinations. Additionally, high variability may result from the dried droplet method (Fig. 3a and b); thus, this may provide a good screening method, but follow-up testing may be required.

Future iterations of the device can be expanded to contain more reactions and microwells and eventually to include more than two sub-wells per microwell. The PDMS microwell array can be designed to contain three or more sub-wells as shown previously[20], which could be useful in screening multiple substrates/enzymes. Some enzymes work synergistically with each other, and testing combinations of three or more droplets (i.e., multiple enzymes and/or multiple substrates) can yield unexpected results.[25] The PDMS microwell array can also be enlarged to include more microwells, further increasing the high-throughput power of Drop-NIMS. Additionally, other target compounds and barcodes may be used, although they would need to be tested to ensure they do not leak from the oil droplets. While the present study demonstrated the characterization of glycoside hydrolases, Drop-NIMS has potential for broad applications in high-throughput characterization of other enzymes important to the food, biofuel, and pharmaceutical industries.

Please do not adjust margins
Lab on a Chip
Page 8 of 9

Author Contributions

Noel Ha: conceptualization, investigation, visualization, writing – original draft. Jenny Onley: conceptualization, data curation, formal analysis, investigation, software, visualization, writing – original draft. Kai Deng: conceptualization, funding acquisition, investigation, writing – review & editing. Peter Andeer: resources. Benjamin P. Bowen: formal analysis, software. Kshitiz Gupta - writing – review & editing. Peter W. Kim: investigation. Nathaniel Kuch: conceptualization, investigation, writing – review & editing. Mark Kutschke: investigation. Alex Parker: investigation. Fangchao Song: investigation. Brian Fox: conceptualization, funding acquisition, project administration, supervision. Paul Adams: conceptualization, funding acquisition, project administration, supervision. Markus de Raad: conceptualization, formal analysis, investigation, software, visualization, writing – original draft. Trent R. Northen: conceptualization, funding acquisition, project administration, supervision, writing – review & editing.

Conflicts of interest

Noel Ha, Markus de Raad, and Trent Northen are inventors on patent US20210102954A1, held by the University of California, covering parts of the method described in this manuscript. Trent Northen is an advisor to Brightseed Bio.

Acknowledgements

Data Availability

OpenMSI files and supplementary data are publicly available under the following filenames and at the coordinating web links.
20210617MdR_5800_NIMS_X2G2xCelEcc.h5
20211021MdR_5800_NIMS_G2X2x4enzymes.h5
20220223MdR_5800_NIMS_Droplet_MSI.h5
20190424MdR_5800_NIMS_Multi_drop_Verapamil_2.h5
20190423MdR_5800_NIMS_Multi_drop_G2_1.h5
https://github.com/biorack/2023_Drop-NIMS.git

References

1   E. E. Kempa, K. A. Hollywood, C. A. Smith and P. E. Barran, *Analyst*, 2019, **144**, 872–891.

2   N. S. Ha, M. de Raad, L. Z. Han, A. Golini, C. J. Petzold and T. R. Northen, *RSC Chem. Biol.*, 2021, **2**, 1331–1351.

3   C. Yu, F. Tang, X. Qian, Y. Chen, Q. Yu, K. Ni and X. Wang, *Sci. Rep.*, 2017, **7**, 4–12.

4   X. Li, R. Yin, H. Hu, Y. Li, X. Sun, S. K. Dey and J. Laskin, *Angew. Chemie - Int. Ed.*, 2020, **59**, 22388–22391.

5   M. J. Jebrail, H. Yang, J. M. Mudrik, N. M. Lafrenière, C. McRoberts, O. Y. Al-Dirbashi, L. Fisher, P. Chakraborty and A. R. Wheeler, *Lab Chip*, 2011, **11**, 3218–3224.

6   R. T. Kelly, J. S. Page, I. Marginean, K. Tang and R. D. Smith, *Angew. Chemie - Int. Ed.*, 2009, **48**, 6832–6835.

7   Y. Zhu and Q. Fang, *Anal. Chem.*, 2010, **82**, 8361–8366.

8   D. Haidas, S. Bachler, M. Kohler, L. M. Blank, R. Zenobi and P. S. Dittrich, *Anal. Chem.*, 2019, **91**, 2066–2073.

9   L. Xu, K. Chang, E. M. Payne, C. Modavi, L. Liu, C. M. Palmer, N. Tao, H. S. Alper, R. T. Kennedy, D. S. Cornett and A. R. Abate, *Nat. Commun.*, 2021, **12**, 6803.

10   V. N. Luk, L. K. Fiddes, V. M. Luk, E. Kumacheva and A. R. Wheeler, *Proteomics*, 2012, **12**, 1310–1318.

11   K. P. Nichols and H. J. G. E. Gardeniers, *Anal. Chem.*, 2007, **79**, 8699–8704.

12   S. K. Küster, S. R. Fagerer, P. E. Verboket, K. Eyer, K. Jefimovs, R. Zenobi and P. S. Dittrich, *Anal. Chem.*, 2013, **85**, 1285–1289.

13   F. Lapierre, G. Piret, H. Drobecq, O. Melnyk, Y. Coffinier, V. Thomy and R. Boukherroub, *Lab Chip*, 2011, **11**, 1620–1628.

14   E. M. Payne, D. A. Holland-Moritz, S. Sun and R. T. Kennedy, *Lab Chip*, 2020, **20**, 2247–2262.

15   H.-K. Woo, T. R. Northen, O. Yanes and G. Siuzdak, *Nat. Protoc.*, 2008, **3**, 1341–1349.

16   E. M. Glasgow, E. I. Kemna, C. A. Bingman, N. Ing, K. Deng, C. M. Bianchetti, T. E. Takasuka, T. R. Northen and B. G. Fox, *J. Biol. Chem.*, 2020, 295, 17752–17769.

17   K. Deng, T. E. Takasuka, R. Heins, X. Cheng, L. F. Bergeman, J. Shi, R. Aschenbrener, S. Deutsch, S. Singh, K. L. Sale, B. A. Simmons, P. D. Adams, A. K. Singh, B. G. Fox and T. R. Northen, *ACS Chem. Biol.*, 2014, **9**, 1470–1479.

18   J. Heinemann, K. Deng, S. C. C. Shih, J. Gao, P. D. Adams, A. K. Singh and T. R. Northen, *Lab Chip*, 2017, **17**, 323–331.

19   A. Kulesa, J. Kehe, J. E. Hurtado, P. Tawde and P. C. Blainey, *Proc. Natl. Acad. Sci. U. S. A.*, , DOI:10.1073/pnas.1802233115.

20   J. Kehe, A. Kulesa, A. Ortiz, C. M. Ackerman, S. G. Thakku, D. Sellers, S. Kuehn, J. Gore, J. Friedman and P. C. Blainey, *Proc. Natl. Acad. Sci. U. S. A.*, 2019, **116**, 12804–12809.

21   R. Chaudhary, T. Kuthiala, G. Singh, S. Rarotra, A. Kaur, S. K. Arya and P. Kumar, *Biomass Convers. Biorefinery*, , DOI:10.1007/s13399-021-01948-2.

22   M. S. Butt, M. Tahir-nadeem, Z. Ahmad and M. T. Sutlan, *Food Technol. Biotechnol.*, 2014, **1**, 22–31.

23   J. Buchert, M. Tenkanen, A. Kantelinen and L. Viikari, *Bioresour. Technol.*, 1994, **50**, 65–72.

24   T. Sawasaki, T. Ogasawara, R. Morishita and Y. Endo, *Proc. Natl. Acad. Sci. U. S. A.*, 2002, **99**, 14652–14657.

25   T. E. Takasuka, J. A. Walker, L. F. Bergeman, K. A. Vander Meulen, S. Makino, N. L. Elsen and B. G. Fox, in *Cell-Free Protein Synthesis: Methods and Protocols*, eds. K. Alexandrov and W. A. Johnston, Humana Press, Totowa,

Lab on a Chip

ARTICLE

NJ, 2014, pp. 71–95.

26 F. W. Studier, *Protein Expr. Purif.*, 2005, **41**, 207–234.

27 B. G. Fox and P. G. Blommel, *Curr. Protoc. Protein Sci.*, 2009, **56**, 139–148.

28 J. A. Walker, T. E. Takasuka, K. Deng, C. M. Bianchetti, H. S. Udell, B. M. Prom, H. Kim, P. D. Adams, T. R. Northen and B. G. Fox, *Biotechnol. Biofuels*, 2015, **8**, 1–20.

29 M. De Raad, T. De Rond, O. Rübel, J. D. Keasling, T. R. Northen and B. P. Bowen, *Anal. Chem.*, 2017, **89**, 5818–5823.

30 W. McKinney, *Proc. 9th Python Sci. Conf.*, 2010, **1**, 56–61.

31 The pandas development team, 2021.

32 R. Vallat, *J. Open Source Softw.*, 2018, **3**, 1026.